THE JOURNAL OF BIOLOGICAL CHEMISTRY VOL. 281, NO. 15, pp. 10496–10507, April 14, 2006

Functional I_{sK}/KvLQT1 Potassium Channel in a New Corticosteroid-sensitive Cell Line Derived from the Inner Ear*

Received for publication, November 15, 2005, and in revised form, January 13, 2006 Published, JBC Papers in Press, February 13, 2006, DOI 10.1074/jbc.M512254200

Marie Teixeira[‡1,2], Say Viengchareun[§¶1], Daniel Butlen[‡], Chrystophe Ferreira[‖], Françoise Cluzeaud[§], Marcel Blot-Chabaud[§], Marc Lombès[§¶], and Evelyne Ferrary[‡3]**

*From the [‡]INSERM EMI-U 0112, Faculté de Médecine Xavier Bichat, [§]INSERM U478, Faculté de Médecine Xavier Bichat, Université Paris 7, 16 rue Henri Huchard, 75870 Paris cedex 18, [¶]INSERM U693, Faculté de Médecine Paris Sud, Université Paris 11, 63 rue Gabriel Péri, 94276, Le Kremlin-Bicêtre, [‖]Institut Fédératif de Recherche Claude Bernard, Faculté de Médecine Xavier Bichat, 16 rue Henri Huchard, 75870 Paris cedex 18, and the **INSERM U608, Faculté de Pharmacie, 27 boulevard Jean Moulin, 13005 Marseille, France*

Endolymph, a high K^+/low Na^+ fluid, participates in mechano-electrical transduction in inner ear. Molecular mechanisms controlling endolymph ion homeostasis remain elusive, hampered by the lack of appropriate cellular models. We established an inner ear cell line by targeted oncogenesis. The expression of SV40 T antigen was driven by the proximal promoter of the human mineralocorticoid receptor (MR) gene, a receptor expressed in the inner ear. The EC5v cell line, microdissected from the semicircular canal, grew as a monolayer of immortalized epithelial cells forming domes. EC5v cells exhibited on filters of high transepithelial resistance and promoted K^+ secretion and Na^+ absorption. Functional MR and the 11β-hydroxysteroid dehydrogenase type 2, a key enzyme responsible for MR selectivity were identified. Expression of the epithelial sodium channel and serum glucocorticoid-regulated kinase 1 was shown to be up-regulated by aldosterone, indicating that EC5v represents a novel corticosteroid-sensitive cell line. Ionic measurements and ^{86}Rb transport assays revealed an apical secretion of K^+ at least in part through the I_{sK}/KvLQT1 potassium channel under standard culture conditions. However, when cells were apically exposed to high K^+/low Na^+ fluid, mimicking endolymph exposure, I_{sK}/KvLQT1 actually functioned as a strict apical to basolateral K^+ channel inhibited by clofilium. Quantitative reverse transcriptase-PCR further demonstrated that expression of KvLQT1 but not of I_{sK} was down-regulated by high K^+ concentration. This first vestibular cellular model thus constitutes a valuable system to further investigate the molecular mechanisms controlling ionic transports in the inner ear and the pathophysiological consequences of their dysfunctions in vertigo and hearing loss.

The inner ear or labyrinth, houses organs responsible for hearing and balance. The organ of Corti, within the cochlea, transduces sounds, whereas the maculae, in the saccule and utricle, and the ampullae of the semicircular canals, transduce linear and angular accelerations, respectively. These complex sensorineural epithelia are composed of sensory hair cells and their supporting cells, and of various nonsensory epithelia. The basolateral side of the membranous labyrinth is bathed by perilymph, an extracellular fluid whose chemical composition is similar to that of plasma and cerebrospinal fluid. Apically, the fluid that bathes the hair bundles of sensory cells is the endolymph that has a unique composition among mammalian extracellular fluids. It is a K^+-rich fluid (170 mM), almost devoid of Na^+ (1 mM), with a lumen positive transepithelial potential. Homeostasis of the volume, pressure, and electrochemical composition of endolymph is pivotal for the transformation of sound into nerve impulse through the apical transduction channels of the sensory hair cells. Thus, dysfunctions in transport systems involved in the homeostasis of K^+ and Na^+ concentrations in endolymph might be responsible for vertigo and hearing loss such as Ménière disease (for review, see Ref. 1).

Cellular models of endolymph secretion by the stria vascularis in the cochlea (for review, see Ref. 2), and by the dark cells in the vestibule, have been proposed, mainly based on *in vitro* studies. It is well established that basolateral Na^+, K^+-ATPase and Na-K-2Cl cotransport are responsible of K^+ entry into the endolymph secretory cells; K^+ is then secreted at the apical side of the cell by a large K^+ conductance, stimulated by DIDS (2), which has been shown to be driven by a I_{sK}/KvLQT1 channel. Furthermore, mutations of *KvLQT1* (KCNQ1) or I_{sK} (KCNE1) are known to cause the Jervell Lange-Nielsen cardioauditory syndrome (3–6) and the invalidation of I_{sK} or *KvLQT1* in mice are responsible for hearing loss due to a lack of transepithelial K^+ secretion (7, 8). Beside K^+ secretion, the maintenance of a low Na^+ concentration in the endolymph is also required for normal functioning of the sensory cells. Only a few studies are related to the transport of sodium in the inner ear. The presence of the epithelial sodium channel (ENaC)[4] has been established in the inner ear, mostly located in the stria vascularis and the Reissner membrane in the cochlea, and at the apical side of the dark cells in the vestibule (9–11).

The location of the cochlea, deep within the temporal bone, combined with the intricate structures of the stria vascularis, render it experimentally difficult to obtain data concerning the molecular mechanisms involved in the *in vivo* production of endolymph and the regulation of its ionic composition. Furthermore, the multicellular organization of the stria vascularis as well as the communication between different cell types, are strong limitations to study these transport systems at the cellular and molecular levels. Until now, only a few cell lines derived from the secretory cells of the inner ear have been characterized (12–

* This work was supported by grants from INSERM, Centre de Recherche Industriel Technique, and from the Bonus Qualite Recherche 2003 of the University Paris 7. The costs of publication of this article were defrayed in part by the payment of page charges. This article must therefore be hereby marked "*advertisement*" in accordance with 18 U.S.C. Section 1734 solely to indicate this fact.

[1] Both authors contributed equally to this paper.

[2] Present address: IFR 128, BioSciences Lyon-Gerland, 21 avenue Tony Garnier, 69007 Lyon, France.

[3] To whom correspondence should be addressed. Tel.: 33-0-1-44-85-62-73; Fax: 33-0-1-42-28-15-64; E-mail: ferrary@bichat.inserm.fr.

[4] The abbreviations used are: ENaC, epithelial sodium channel; MR, mineralocorticoid receptor; TAg, large T antigen; PBS, phosphate-buffered saline; GR, glucocorticoid receptor; HPLC, high pressure liquid chromatography; ANOVA, analysis of variance; 11β-HSD2, 11β-hydroxysteroid dehydrogenase type 2; RT, reverse transcriptase; DIDS, 4,4′-diisothiocyanostilbene-2,2′-disulfonic acid.

14), and, probably because of the high specificity of these cells and their dedifferentiation in culture, no main results have been subsequently published following the first characterization of these cell lines. To circumvent these difficulties, we developed a new immortalized cell line from the ampulla of the semicircular canal. In this structure, in contrast to the cochlea, the endolymph secretory cells are the dark cells that form a single cell type monolayer; the composition of endolymph (with the exception of the high positive endocochlear potential), and the transport systems involved in endolymph secretion are similar to those described in the cochlea (15).

Because several immunocytochemical studies and steroid binding assays have suggested that the mineralocorticoid receptor (MR) was expressed in the inner ear (16), we used a targeted oncogenesis strategy in transgenic mice using the proximal P1 promoter of the human MR (hMR) gene to drive expression of the immortalizing SV40 large T antigen (TAg) in this tissue. Thus, our transgenic animals enabled us to derive several novel cell lines originating from normally MR-expressing tissues, including brown fat, brain, lung, sweat glands, liver, and kidney (17).

In the present study, we characterized the EC5v cell line that constitutes to our knowledge the first differentiated cellular model derived from the ampulla of the semicircular canal. We aimed at deciphering at the cellular and molecular levels the mechanisms involved in the homeostasis of K^+ and Na^+ in endolymph. We showed that this new cellular model expressed mineralocorticoid and glucocorticoid receptors and that vestibular cells are direct targets of corticosteroid hormone actions. Interestingly, EC5v cells are highly differentiated polarized epithelial cells that generated a high transepithelial resistance and promoted K^+ secretion and Na^+ absorption. We also demonstrated the presence of a functional apical I_{sK}/KvLQT1 potassium channel that is implicated in K^+ secretion under standard culture conditions but more importantly is involved in the maintenance of the high K^+ gradient when the apical side of cells were exposed to high K^+, low Na^+ endolymph-like fluid. Under these physiological asymmetric culture conditions, steady state levels of KvLQT1 mRNA were drastically reduced, underlying an unrecognized transcriptional control of this potassium channel expression by extra- and intracellular ionic composition of the inner ear.

EXPERIMENTAL PROCEDURES

Generation of Transgenic Mice by Targeted Oncogenesis—P1-TAg transgene containing the immortalizing SV40 large T Antigen (TAg) under the control of the proximal promoter (P1) of the human mineralocorticoid receptor gene was generated as previously described (18, 19). Microinjections into fertilized oocytes derived from B6D2F1 mice were realized at the "Plateau de Transgenèse" of the Institut Fédératif de Recherche Claude Bernard (Faculté de Médecine Xavier Bichat, Paris, France). Founders were identified by PCR analyses of tail DNA from 2-week-old mice using oligonucleotides specific for the SV40 TAg (sense primer S5108, 5′-TTGAAAGGAGTGCCTGGGGGAAT-3′; antisense primer A4920, 5′-CAGTTGCATCCCAGAAGCCTCCA-3′); PCR conditions are available upon request.

Establishment of the EC5v Cell Line—Several cell lines were derived from the inner ear of a 4-week-old transgenic mouse. In particular, the ampulla of the semicircular canal, the lateral wall, the stria vascularis, and the organ of Corti were microdissected under a microscope, transferred into a collagen I-coated 12-well plate (Institut J. Boy, Reims, France), and cultured in the following medium: Dulbecco's modified Eagle's/Ham's F-12 medium (1:1), 20 mM HEPES, pH 7.4, 100 units/ml penicillin, 100 μg/ml streptomycin, 2 mM glutamine, and 20% fetal calf serum (Invitrogen). This medium was removed every 2 days for 2 weeks, until the appearance of a monolayer of cells, which were selected for their epithelioid morphology and the immunodetection of the SV40 TAg in their nucleus. Among these cells, the EC5v cell line, originating from the ampulla of the semicircular canal, was further characterized. The EC5v cell line was subcloned by limited dilution to obtain a homogeneous cell population and was routinely cultured at 37 °C in a humidified incubator gassed with 5% CO_2 within an epithelial medium composed of Dulbecco's modified Eagle's/Ham's F-12 medium (1:1), 2 mM glutamine, 50 nM dexamethasone (Sigma), 50 nM sodium selenite (Sigma), 5 μg/ml transferrin, 5 μg/ml insulin (Sigma), 10 ng/ml epidermal growth factor (Tebu, Le Perray en Yvelines, France), 2 nM triiodothyronine (Sigma), 100 units/ml penicillin, 100 μg/ml streptomycin, 20 mM HEPES, pH 7.4, and 2% fetal calf serum. EC5v cells were utilized from passage 30 to 40.

Hormones, Drugs, and Chemicals—Aldosterone was purchased from Acros Organics (Noisy le Grand, France), whereas amiloride, bumetanide, mifepristone (RU486), ouabain, and spironolactone were purchased from Sigma. Clofilium tosylate was obtained from ICN Biochemicals Inc. Other reagents were purchased from Invitrogen, except when stated.

Cell Culture—EC5v cells were seeded on either collagen I-coated Transwell/Snapwell filters (Costar Corp., Brumath, France) or collagen I-coated Petri dishes with the epithelial medium. To study corticosteroid actions, epithelial medium was replaced by a minimum medium having the same composition as the epithelial medium with omission of dexamethasone and fetal calf serum. For some experiments, the medium bathing the apical surface of the cells cultivated on Transwell filters was replaced by an artificial endolymphatic medium composed of 1.8 mM $CaCl_2$, 1.2 mM $MgCl_2$, 35 mM $KHCO_3$, 125 mM KCl, and 5 mM glucose, pH 7.4.

Immunocytochemical Analyses—Cells were generally cultured on glass coverslides, fixed with 4% paraformaldehyde in PBS for 10 min, rinsed for 5 min with PBS, and then permeabilized by 0.1% Triton X-100 in PBS for 10 min. The presence of the SV40 TAg protein was detected in the nucleus using a 1:10 dilution of the monoclonal anti-SV40 TAg antibody (Ab-2; Calbiochem, La Jolla, CA). Pan-cytokeratins (C2562, Sigma), α1 Na^+, K^+-ATPase, ZO-1, I_{sK} (gift of J. Barhanin), and KvLQT1 (gift of J. Barhanin) immunodetection was performed on cells cultivated onto Transwell filters, incubated overnight at 4 °C with 1:200, 1:50, 1:250, 1:2000, and 1:500 primary antibody dilutions, respectively. Secondary antibodies (Alexa 546 goat anti-rabbit, or Alexa 533 goat anti-mouse (Molecular Probes, Cergy-Pontoise, France) were used at a 1:200 dilution and incubated 1 h at room temperature. Micrographs of these immunocytochemical analyses were obtained with a Zeiss LSM510 confocal microscope.

Electron Microscopic Analyses—EC5v cells were grown on Transwell filters with complete epithelial medium. Cells were then rinsed with PBS and fixed for 30 min with 2.5% glutaraldehyde in PBS at room temperature. Cells were rinsed in PBS, postfixed with 1% osmic acid for 15 min, dehydrated in graded ethanol, and embedded in EPON 812 (Fluka, St. Quentin, France). Ultrathin sections were realized on transversely oriented confluent cells and examined with a Jeol JEM 1010 electron microscope.

Western Blot Analyses—Total protein extracts were prepared from EC5v cells cultured in the epithelial medium on collagen I-coated Petri dishes or Transwell filters. Briefly, cells were washed twice with iced-cold PBS and lysed on ice with 10 mM Tris-HCl, pH 7.6, 5 mM EDTA, 150 mM NaCl, 30 mM sodium pyrophosphate, 50 mM sodium fluoride, 1 mM sodium orthovanadate, 10% glycerol, and 2% Nonidet P-40 supplemented, just before use, with 1 μM pepstatin A, 50 μM leupeptin, 1 μM

TABLE 1

Primer sequences of genes analyzed in RT-PCR and real time PCR

The abbreviations of the genes, their full name, their GenBank accession number and 5′ to 3′ nucleotide sequences of the sense and antisense primers are presented.

Name	Accession number	Amplicon	Sense primer	Antisense primer
Primers for RT-PCR				
I_{sK}	X60457	296 bp	GCTCGTAAGTCTCAGCTCCG	CGACAATGGCTTCAGTTCAGG
KvLQT1	U70068	439 bp	CCCTCTTCTGGATGGAGAT	ATCTGCGTAGCTGCCAAAC
mGR	X04435	320 bp	ATATTTGCCAATGGACTCCAAAG	GTTTCGGTCTCTCCCATATACA
11β-HSD2	BC066209	474 bp	TGACGTGGGACTGTCTCCAGT	CTGAGCTGCCAGCAATGCATCGAT
αENaC	AF112185	555 bp	CTAATGATGCTGGACCACACC	AAAGCGTCTGTTCCGTGATGC
βENaC	AF112186	631 bp	GCCAGTGAAGAAGTACCTGC	CCTGGGTGGCACTGGTGAA
γENaC	AF112187	670 bp	AAGAATCTGCCGGTTCGAGGC	TACCACTCCTGGATGGCATTG
Primers for real time PCR				
18 S	X00686	66 bp	CCCTGCCCTTTGTACACACC	CGATCCGAGGGCCTCACTA
I_{sK}	X60457	150 bp	ACCCTTTCAACGTGTACATCGA	TTCAGTTCAGGAAGGTGTGTGG
KvLQT1	U70068	150 bp	GCTGAGAAAGATGCGGTGAAC	AGAAACAGGAGGCGATGGTCT
mMR	M36074	153 bp	ATGGAAACCACACGGTGACCT	AGCCTCATCTCCACACACCAAG
αENaC	AF112185	150 bp	GGACTGGAAAATCGGCTTCC	TAGAGCAGGCGAGGTGTCG
Sgk1	AF205855	150 bp	TCACTTCTCATTCCAGACCGC	ATAGCCCAAGGCACTGGCTA

aprotinin, and 1 mM phenylmethylsulfonyl fluoride. Lysates were sonicated and cleared from insoluble material by centrifugation. Protein concentrations were determined by the modified Bradford method and 60 μg of total protein were directly submitted to SDS-PAGE. After protein blotting on a polyvinylidene difluoride membrane, blots were incubated overnight in 5% milk-Tris buffer saline, 0.1% Tween before incubation with the rabbit anti-α, -β, -γ ENaC antibodies (1:5000), with the rabbit anti-I_{sK} (1:750) or with the rabbit anti-KvLQT1 antibody (1:500) for 1 h at room temperature. After extensive washes, membranes were incubated with a goat peroxidase-conjugated second antibody (1:8000) for 1 h at room temperature and proteins were visualized by use of the ECL$^+$ detection kit (Amersham Biosciences).

Whole Cell Binding Assays—Specific binding of [^{3}H]aldosterone and [^{3}H]dexamethasone was determined in EC5v cells grown on a collagen I-coated 12-well plate. Cells were grown for 48 h in epithelial medium before incubation overnight in minimum medium. Then, cells were incubated for 1 h, at 37 °C, with 10 nM [^{3}H]aldosterone (1739 GBq/mmol; Amersham Biosciences), or with 50 nM [^{3}H]dexamethasone (1517 GBq/mmol; Amersham Biosciences) in the presence or absence of a 100-fold excess of the MR antagonist spironolactone or glucocorticoid receptor (GR) antagonist RU486. Cells were rinsed with cold 1× PBS before steroid extraction by the addition of cold ethanol (200 μl followed by 100 μl). Radioactivity of the ethanol extracts was measured with a liquid scintillation β counter (Wallac Pharmacia, Orsay, France). Specific [^{3}H]steroid binding was determined from the difference between total and nonspecific binding and was expressed as femtomole/mg of protein.

Measurement of the 11β-Hydroxysteroid Dehydrogenase Type 2 Catalytic Activity—EC5v cells were seeded at 6×10^5 cells per well on a collagen I-coated 12-well plate and cultured for 48 h in epithelial medium before incubation overnight in minimum medium. To permeabilize cells, plates were frozen at −80 °C and thawed at room temperature (3 cycles). Then, EC5v cells were incubated at 37 °C with 10 nM [^{3}H]corticosterone (B) (2590 GBq/mmol; Amersham Biosciences) in the presence or absence of 1 mM NAD or NADP (Roche Molecular Biochemicals). Time-dependent production of [^{3}H]dehydrocorticosterone (A) was measured by HPLC as previously described (20 μl of supernatant was collected and 80 μl of HPLC mobile phase (methanol/H_2O, 1:1) containing 100 nM unlabeled corticosterone and 11-dehydrocorticosterone as internal standards were added). The amount of steroid metabolite generated per well was normalized by the amount of protein, determined by the Bradford method after homogenization of cells in the lysis buffer. Results are expressed as femtomoles of 11-dehydrocorticosterone produced per hour per microgram of protein per well (fmol/h/μg of protein).

RT-PCR—Total RNA was extracted from cells with TRIzol reagent according to the manufacturer's recommendations and RNA were thereafter processed for RT-PCR. Briefly, 2 μg of total RNA was treated using the DNase I Amplification Grade procedure. RNA was then reverse-transcribed with 200 units of reverse transcriptase using the Superscript^{TM} II kit according to the manufacturer's recommendations using random hexamers (Promega). PCR were performed with a thermocycler (Stratagene, Paris, France) in a final volume of 25 μl, in 1× PCR buffer containing 1.5 mM $MgCl_2$, 10 pmol of sense and antisense primers, 200 μM dNTP, 1 unit of *Taq* Platinum, and 2 μl of the reverse transcription reaction. The PCR cycles were as followed: 95 °C for 5 min, specific hybridization temperature for 1 min, 72 °C for 1 min, during 1 cycle; 95 °C for 45 s, specific hybridization temperature for 45 s, 72 °C for 45 s, during 30 cycles; 72 °C for 7 min, during 1 cycle. Amplicons were thereafter separated onto 2% agarose gels and visualized under UV excitation. Table 1 indicates primer sequences of genes analyzed by PCR and quantitative real-time PCR.

Quantitative Real Time PCR—Specific gene expression was quantified by real time PCR. Total RNA, extracted as described above, was processed for real time PCR carried out on an ABI 7700 Sequence Detector (Applied Biosystems, Foster City, CA). Briefly, 1 μg of total RNA was treated using the DNase I Amplification Grade procedure. The amount of total RNA present in each sample was thereafter measured by the Ribogreen kit (Interchim). RNA was then reverse-transcribed as described above. Samples were diluted 10-fold, then 1/20 of the reverse transcription reaction was used for PCR using the qPCR^{TM} Mastermix Plus for Sybr^{TM} Green I (Eurogentec, Seraing, Belgium). PCRs were performed in the presence of 2.5 mM $MgCl_2$, 200 μM dNTPs, and 1.25 unit of Hot Goldstar DNA polymerase. Final primer concentrations were 300 nM for each primer (see Table 1). PCR reagents were from Eurogentec. Reaction parameters were 50 °C for 2 min followed by 40 cycles at 95°C for 15 s, and 60 °C for 1 min. For preparation of standards, amplicons were purified from agarose gel and subcloned into pGEMT-easy plasmid (Promega), then sequenced to confirm the identity of each fragment. Standard curves were generated using serial dilutions of linearized standard plasmids, spanning 5 orders of magnitude and yielding correlation coefficients >0.98 and efficiencies of at least 0.95, in all experiments. Standard and sample values were determined in duplicate from independent experiments. Relative expression within a given sample was calculated as the ratio: attomoles of specific gene/femtomol of 18 S. Results are mean ± S.E. and present the relative

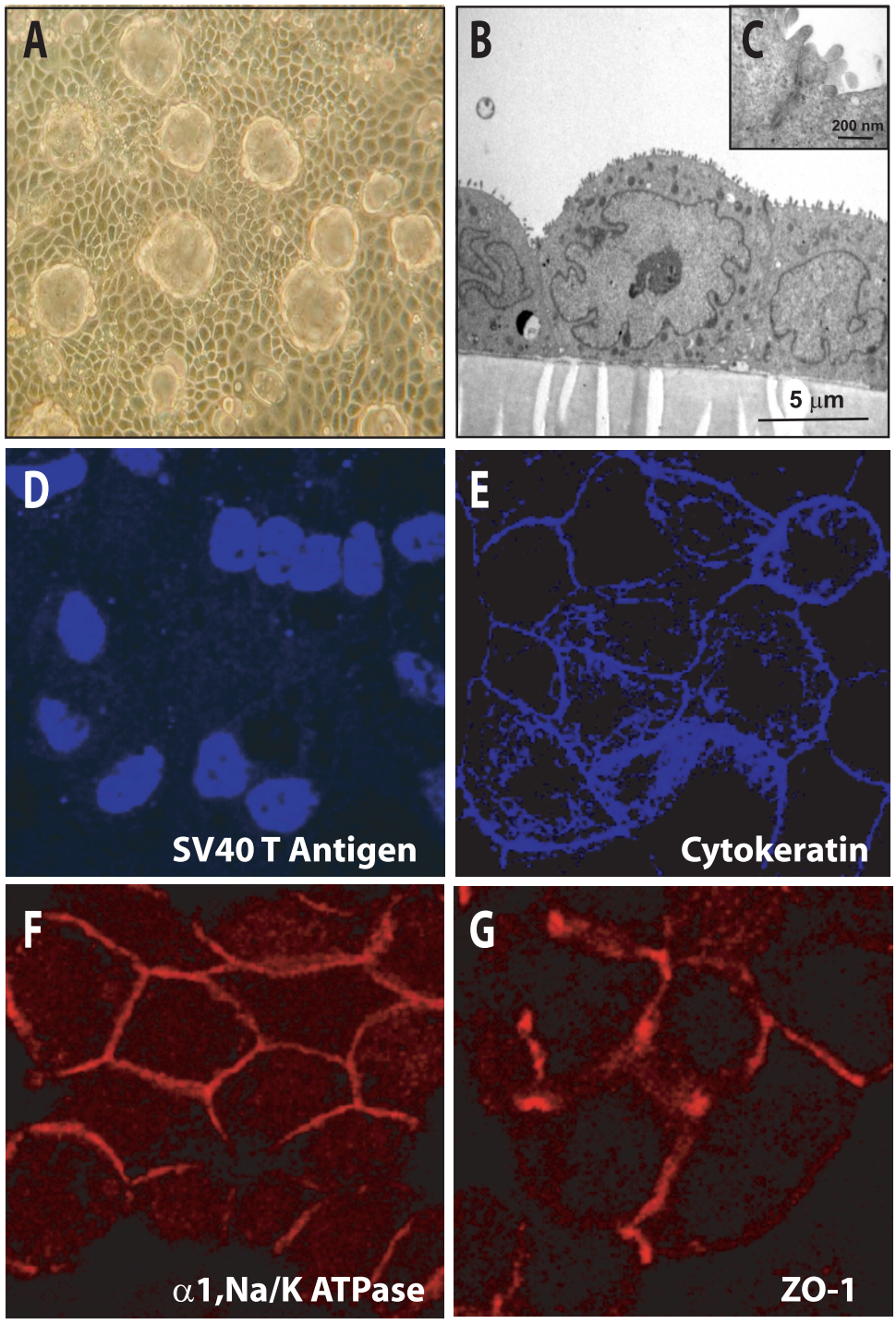

FIGURE 1. **Morphological and functional features of the vestibular EC5v cells.** EC5v cells, originating from semicircular canals of the inner ear of a P1-TAg transgenic mouse, were maintained in the epithelial medium described under "Experimental Procedures" in a saturated 5% CO_2, 95% air atmosphere at 37 °C. *A*, phase-contrast micrograph (*left panel*) of confluent EC5v cells grown on a Petri dish coated with collagen I (passage 33). Note the presence of multiple domes indicating that hydroelectrolytic transports take place across these cells (optical lens × 20). *B* and *C*, electron microscopic micrographs (*B*) of EC5v cells grown on filters forming monolayers of epitheloid cells and presenting microvilli at the apical side of the membrane and tight junctions (*inset C*). *D–G*, immunocytochemistry detection of the SV40 large T antigen as a strong nuclear staining (*D*), pancytokeratins (*E*), α1 Na^+, K^+-ATPase (*F*), and the tight junction associated protein ZO-1 (*G*) (optical lens ×63).

expression compared with that obtained with control cells, which was arbitrary set at 1.

Electrophysiologic Studies—The measurement of the short-circuit current (Isc, $\mu A/cm^2$), transepithelial potential (V_T, mV), and transepithelial resistance (R_T, $\Omega \times cm^2$) were performed on EC5v cells grown on collagen I-coated Snapwell filters as described previously (20). Briefly, Snapwell filters were incubated overnight in epithelial medium. They were then mounted into a voltage clamp system (Costar Corp.). Cells were bathed on each side with 8 ml of epithelial medium thermostated at 37 °C. At time 0, the drug was added at the apical or the basolateral side of the filter; in some experiments, the apical medium was replaced by an endolymph-like solution (K = 160 mM). After a 30-min period, the voltage current clamp was used to measure Isc by clamping the transepithelial potential to 0 mV for 1 s.

Ions Measurements—Cells were seeded on collagen I-coated Transwell filters and were cultured for 5 days in the epithelial medium. Thereafter, medium was replaced for 24 h by fresh epithelial medium with or without drugs. In some experiments, the apical medium was an endolymph-like solution (see above). The day after, 400 μl of the supernatant was recovered from the medium bathing the apical and basolateral surface of the EC5v cells. K^+, Na^+, and Cl^- ions were thereafter measured by the "Centre d'Expérimentation Fonctionnelle Intégrée" of the IFR Claude Bernard on an Olympus automate.

^{86}Rb Transport—EC5v cells (~10^6) were seeded on Transwell filters (12 mm diameter) and cultured for 5 days in the epithelial medium. The day of the experiment, medium was removed and replaced with fresh medium containing 185 kBq/well of ^{86}Rb (Amersham Biosciences, 18.5–370 MBq/mg of Rb), either in the basolateral (1.5 ml) or apical (0.5 ml) compartment. The time course of Rb flux was evaluated by sampling 5 μl at 15, 30, 45, 60, 90, and 120 min at the apical or basolateral sides for determination of basolateral to apical flux and apical to basolateral flux, respectively. For each filter, radioactivity was determined in duplicate. In some experiments, at $t = 0$, drugs were added at the basolateral or apical side of the epithelium. Radioactivity was counted by scintillation counting in 2 ml of scintillation liquid (Lumagel, Lumac-LSC). Fluxes (nmol/cm^2) were calculated as a function of the K^+ concentration and the specific radioactivity, assuming that Rb^+ is a strict marker of K^+ and corrected for the filter area. Results are expressed as the mean of at least 6 independent filters.

Statistical Analyses—Data are expressed as the mean ± S.E. Student's *t* test or analysis of variance with Dunnett's multiple comparison post-test (indicated as ANOVA) were used to determine significant differences among groups. Regression line slopes were compared by *t* test. Statistical significance was achieved for a p value ≤0.05.

RESULTS

Generation of the EC5v Cell Line and Morphological Features of the Cells—By using a targeted oncogenesis strategy, we were able to generate a new cell line derived from microdissected ampulla of a transgenic mouse. Confluent EC5v cells grown on plastic support were cuboid and formed numerous domes (Fig. 1*A*). Electron microscopic analyses revealed that these cells formed a monolayer of epithelial cells, when grown on filters (Fig. 1*B*), and presented tight junctions, desmosomes, and apical microvilli, which are typical features of polarized cells (Fig. 1*C*). Immunocytochemical studies also indicated that EC5v cells presented a typical network of cytokeratins (Fig. 1*E*) and the tight junction-associated protein ZO-1 at the cell periphery (Fig. 1*G*). Moreover, confocal laser scanning microscopy indicated that EC5v cells expressed the α1 Na^+,K^+-ATPase (Fig. 1*F*). As expected, we showed that this cell line was immortalized by the SV40 TAg, as revealed by the immunodetection of this oncoprotein in the nuclear compartment of cells (Fig. 1*D*).

Molecular Characterization of the Transport Systems in EC5v Cells—We first examined the expression of genes known to be involved in potassium transport in the inner ear. In particular, we analyzed by RT-PCR whether EC5v cells expressed transcripts of the I_{sK}/KvLQT1 potassium channel. As shown in Fig. 2, *A* and *B* (*left panels*), a 296-bp amplicon for I_{sK} and a 439-bp amplicon for KvLQT1 were detected in EC5v cells. Western blot analysis provided evidence that I_{sK} proteins were also detected as ~17-, 27-, and 35-kDa species (Fig. 2*A*, *right panel*). It is worth noting that the culture conditions, *i.e.* filter *versus* Petri dish, seem to influence the relative ratio between protein band species that are likely to correspond to various glycosylated forms of I_{sK} (21). In addition, KvLQT1 was also detected in these cells by confocal microscopy experiments, as presented in Fig. 2*B* (*right panel*) with a cytoplasmic and/or submembrane staining. Interestingly, the three subunits of ENaC were also expressed at both mRNA (Fig. 2*C*, *left panels*) and protein levels (Fig. 2*C*, *right panels*) indicating that EC5v are epithelial cells that possess all the molecular elements required to ensure both potassium and sodium transport.

EC5v Cells Are Sensitive to Corticosteroid Hormone Action—Because EC5v cells were generated by a targeted oncogenesis strategy through utilization of the proximal promoter of the human mineralocorticoid receptor gene, we anticipated that the endogenous expression of MR might be maintained in these cells as we first detected by RT-PCR transcripts of the murine MR (Fig. 3*A*). Competition studies, using 100-fold excess of unlabeled aldosterone and spironolactone, a mineralocorticoid antagonist, enabled identification of these specific [^{3}H]aldosterone binding sites as mineralocorticoid receptors, estimated at 20 fmol/mg of protein (Fig. 3*B*). In addition, Scatchard plot analysis of aldosterone

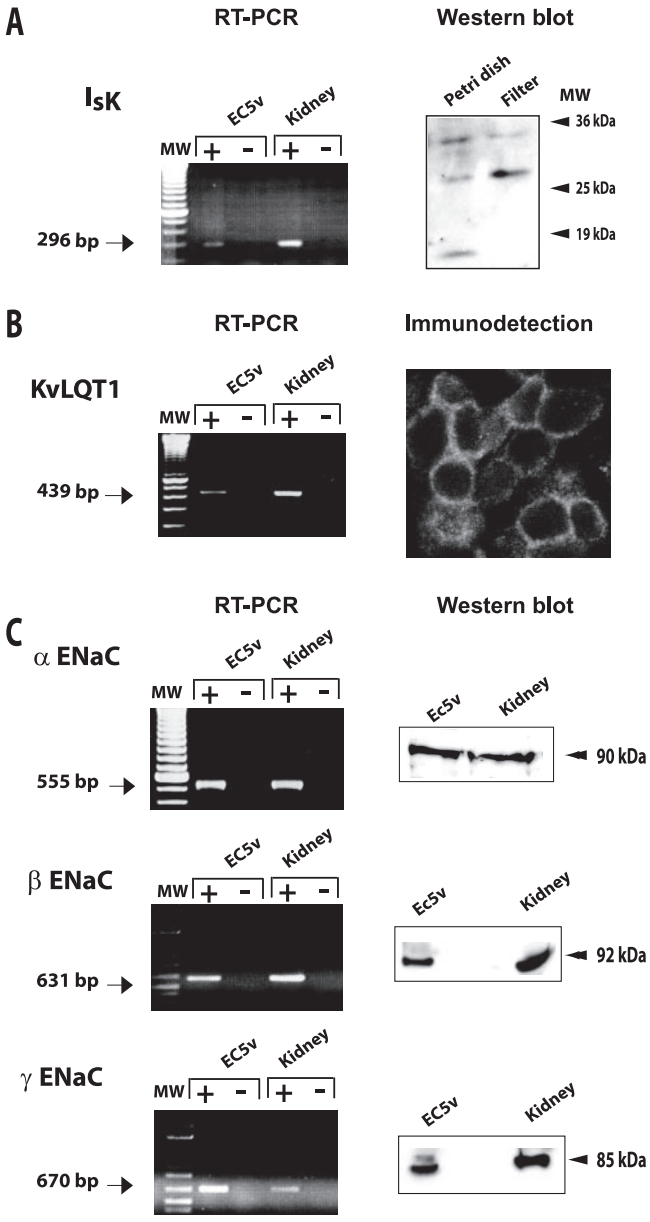

FIGURE 2. **Molecular characterization of EC5v cells.** *A*, identification of I_{sK}. RT-PCR analysis as used for total RNA extracted from EC5v cell passage 15 and wild-type mouse whole kidney, as positive control, were reverse-transcribed with random primers in the presence (+) or absence (−) of the reverse transcriptase. cDNA were then amplified as described under "Experimental Procedures." RT-PCR experiments allowed detection of a 296-bp amplicon amplified with specific primers (*left panel*). Western blot analysis was used for 60 μg of cell lysate protein submitted to SDS-PAGE and blotted with an anti-I_{sK} antibody (*right panel*). Three bands at 17, 27, and 35 kDa were identified in EC5v cell lysate. Note that the 27-kDa species seemed to be more intensively expressed when the cells were grown onto filters. *B*, identification of KvLQT1. RT-PCR experiments allowed detection of a 439-bp amplicon amplified with specific primers (*left panel*). Immunocytochemical detection of KvLQT1, observed with a confocal microscopy, is illustrated on the *right panel*. *C*, expression of the three subunits of the ENaC. RT-PCR were performed as described above and allowed the detection of a 555-(α ENaC), 631-(β ENaC), and a 670-bp (γ ENaC) amplicon. Western blot analysis was performed as described above and allowed the detection of the three subunits of ENaC at 90 (α ENaC), 92 (β ENaC), and 85 kDa (γ ENaC). Whole kidney homogenate was used as positive control.

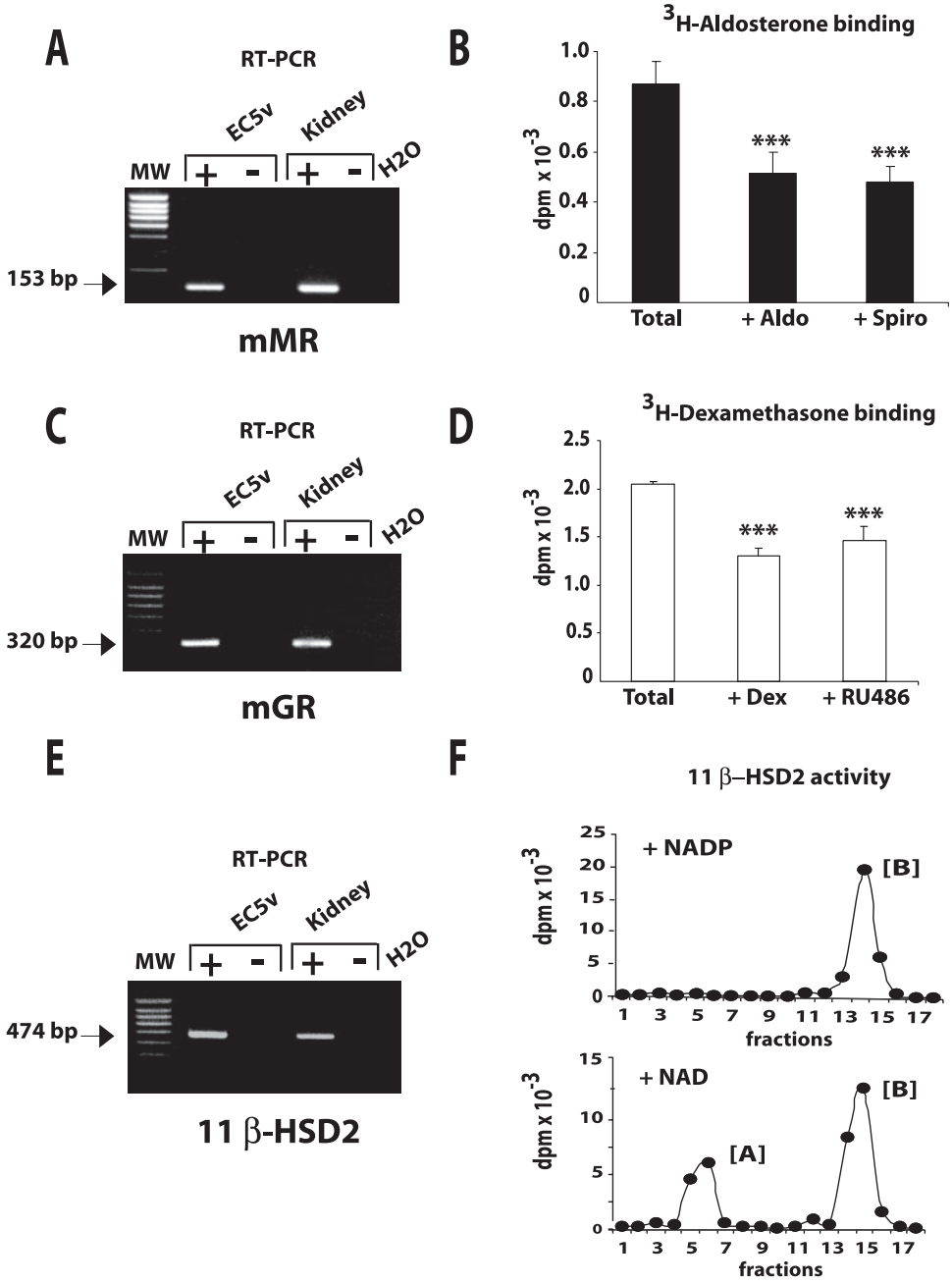

FIGURE 3. **Mineralocorticoid and glucocorticoid receptor expression in EC5v cells.** Total RNA extracted from EC5v cells and from whole kidney used as positive controls was reverse-transcribed as described above and cDNA were submitted to PCR with specific primers for mouse MR (*A*) or mouse GR (*C*) with RT-PCR. For whole cell binding of [^{3}H]corticosteroid in EC5v cells, cells were incubated in steroid-free medium 24 h prior to the experiment. For the aldosterone binding assay, 10 nM [^{3}H]aldosterone, with and without a 100-fold excess of unlabeled aldosterone (+*Aldo*), or spironolactone (+*Spiro*), was added (*B*). For the dexamethasone binding assay, 50 nM [^{3}H]dexamethasone, with and without a 100-fold excess of unlabeled dexamethasone (+*Dex*) or RU486 (+*RU486*), was added to cells (*D*). After a 1-h incubation at 37 °C, cells were rinsed twice with ice-cold PBS, lysed with cold ethanol, and the radioactivity counted. Data represent mean ± S.E. of three independent determinations. The MR and GR levels were estimated at 20 and 48 fmol/mg of protein, respectively. ***, statistical significance compared with the total binding, $p < 0.001$. *E*, a specific 11-β-HSD2 transcript was detected by RT-PCR in EC5v cells (474 bp). *F*, catalytic activity of 11β-HSD2 in EC5v cells. Cells were incubated for 1 h with 10 nM [^{3}H]corticosterone (*B*), and time-dependent production of [^{3}H]dehydrocorticosterone (*A*) was measured by HPLC and the radioactivity of each fraction was counted. Cofactor specificity of 11β-HSD2 dehydrogenase activity was assessed in permeabilized EC5v cells after incubation with 10 nM [^{3}H]corticosterone (*B*) in the presence of 1 mM NADP (*upper panel*) or 1 mM NAD (*lower panel*). The catalytic activity of 11β-HSD2 in the presence of NAD was calculated at 5.9 fmol of [^{3}H]dehydrocorticosterone (*A*) formed per mg/protein per h.

binding to the cytosolic fraction of EC5v cells revealed the high affinity of aldosterone for its specific sites with a calculated K_d at 0.37 ± 0.10 nM (data not shown). Fig. 3*C* shows that GR were also expressed in EC5v cells as revealed by RT-PCR. Tritiated dexamethasone binding in EC5v was partially competed by 100-fold excess of unlabeled dexamethasone and RU486, a glucocorticoid antagonist. The estimated GR concentration was 48 fmol/mg of protein (Fig. 3*D*). Finally, we examined whether the 11β-hydroxysteroid dehydrogenase type 2 (11β-HSD2), an enzyme involved in the mechanisms conferring mineralocorticoid receptor selectivity, was present in these epithelial cells. We showed that EC5v cells expressed 11β-HSD2 at both mRNA and enzymatic levels, because a metabolic conversion of corticosterone (compound B) to 11 dehydrocorticosterone (compound A) was detected in these cells (Fig. 3, *E* and *F*). The NAD dependence of the dehydrogenase activity indicated that it corresponds to the form responsible for MR selectivity with a calculated catalytic activity at 5.9 fmol/h/μg of protein, a relatively high activity, although at a 10 times lower level than that measured in the prototypic aldosterone target cells of the distal nephron (17).

EC5v Cells Secrete Potassium via a Na$^+$, K$^+$-ATPase and Na-K-2Cl Cotransport-dependent System—To test the ability of these EC5v cells to secrete K$^+$ via basolateral Na$^+$, K$^+$-ATPase and Na-K-2Cl cotransport, cells were cultured on filters, in the presence of low K$^+$ concentration (4.2 mM) on both sides. In these conditions, EC5v cells developed a high transepithelial resistance (1421 ± 72.7 Ω × cm^2, $n = 35$). After 24 h, a difference in K$^+$ concentration was observed between the two compartments. The K$^+$ gradient calculated as apical − basolateral concentrations was 1.5 ± 0.07 mM, $n = 30$, and 2.4 ± 0.08 mM, $n = 25$, after 24 and 48 h, respectively (Fig. 4*A*). An inverted Na$^+$ gradient was generated (calculated as apical − basolateral Na$^+$ concentrations: −1.8 ± 0.30 mM, $n = 30$ and −2.0 ± 0.24 mM, $n = 25$, after 24 and 48 h,

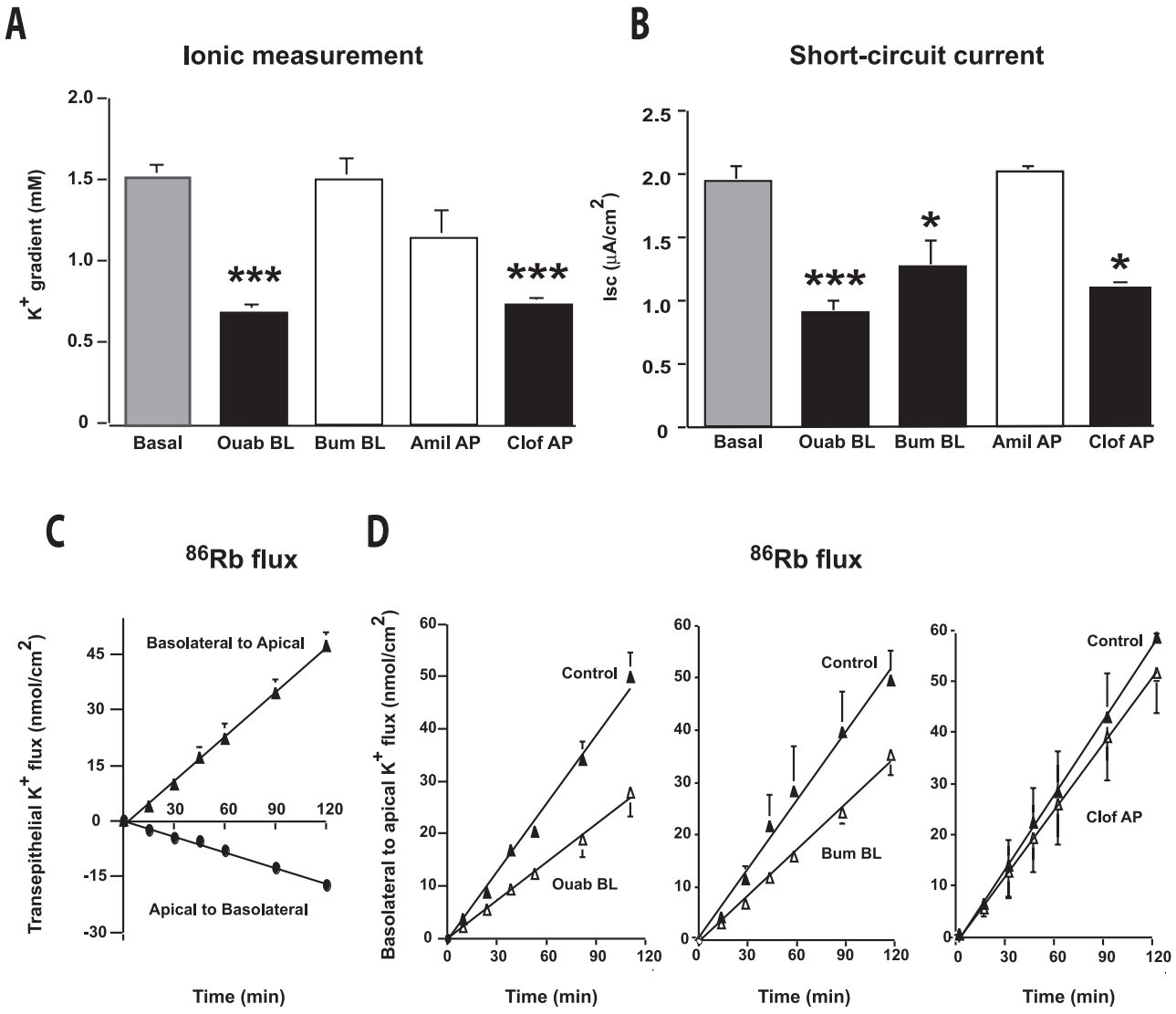

FIGURE 4. **Characterization of potassium transport in EC5v cells with both sides bathed with low K^+ concentration.** In these series of experiments, cells were cultured on filters, in a low K^+ medium (4.2 mM) on both sides. Ouabain (*Ouab*, 10^{-4} M, inhibitor of the Na^+, K^+-ATPase) and bumetanide (*Bum*, 10^{-4} M, inhibitor of the Na-K-2Cl cotransport) were added to the basolateral compartment (*BL*); amiloride (*Amil*, 10^{-5} M, inhibitor of ENaC) and clofilium (*Clof*, 10^{-4} M, inhibitor of I_{sK}/KvLQT1 channel) were added to the apical (*AP*) compartment. *A*, secretion of K^+. When the cells were cultured on filters for a 24-h period, they were able to secrete K^+ and generated a K^+ gradient (Basal: 1.5 ± 0.07 mM, $n = 30$) with a higher K^+ concentration in the apical side than in the basolateral one. This gradient was lower in the presence of basolateral ouabain and apical clofilium (ANOVA, ***, $p < 0.001$). Basolateral bumetanide and apical amiloride did not alter this gradient. *B*, short-circuit current. In basal conditions, the short-circuit current was 1.9 ± 0.13 μA/cm² ($n = 12$). This current was decreased by a 30-min application of basolateral ouabain or bumetanide or apical clofilium (ANOVA, *, $p < 0.05$; ***, $p < 0.001$). Apical amiloride did not alter Isc. *C*, calculated unidirectional transepithelial K^+ flux with ^{86}Rb determination in basal conditions. When ^{86}Rb was added in the basolateral compartment and measured in the apical one (basolateral to apical flux), the radioactivity increased in the apical compartment as a function of time following the equation: $y = 0.40\,x - 1.25$ ($r^2 = 0.998$, means of 39 independent determinations), where y is in nanomole/cm² and x is in minutes. On the opposite, when ^{86}Rb was added in the apical compartment and measured in the basolateral one (apical to basolateral flux), the radioactivity increased in the basolateral compartment as a function of time following the equation: $y = 0.14\,x - 0.14$ ($r^2 = 0.992$, means of 18 independent determinations), where y is in nanomole/cm² and x is in minutes. *D*, calculated basolateral to apical transepithelial K^+ flux with ^{86}Rb determination in the presence of transporter inhibitors. In the presence of ouabain or bumetanide, applied in the basolateral compartment, a clear decrease of the K^+ flux was observed. The calculated curves for basolateral to apical K^+ flux were $y = 0.42\,x - 2.30$ ($r^2 = 0.991$) and $y = 0.23\,x - 0.93$ ($r^2 = 0.994$) for control and ouabain-treated cells, respectively (means of 18 independent determinations, difference between the slopes: $p < 0.025$); $y = 0.44\,x - 0.36$ ($r^2 = 0.988$) and $y = 0.30\,x - 1.55$ ($r^2 = 0.994$) for control and bumetanide-treated cells, respectively (means of 15 independent determinations, difference between the slopes: $p < 0.05$); $y = 0.49\,x - 0.74$ ($r^2 = 0.999$) and $y = 0.43\,x - 0.68$ ($r^2 = 0.994$) for control and clofilium-treated cells, respectively (means of 9 independent determinations, slopes non-significantly different), where y is in nanomole/cm² and x is in minutes.

respectively). These results strongly suggest K^+ secretion from the basolateral to the apical side of this polarized epithelium. This vectorial K^+ secretion, associated with Na^+ absorption, was partially inhibited by ouabain (10^{-4} M), an inhibitor of the Na^+,K^+-ATPase applied in the basolateral compartment for 24 h (K^+ gradient: 0.68 ± 0.047 mM, $n = 18$, ANOVA, $p < 0.001$; Na^+ gradient: −0.47 ± 0.311 mM, $n = 18$, ANOVA, $p < 0.05$). No effect of the inhibitor of the Na-K-2Cl cotransport, bumetanide (10^{-4} M), was observed (Fig. 4*A*) when added in the basolateral compartment. Apical administration of ouabain or bumetamide has no significant effect on K^+ transport (K^+ gradient: 1.6 ± 0.19, $n = 6$; 1.6 ± 0.21, $n = 6$, respectively). Amiloride (10^{-5} M), an inhibitor of ENaC, did not significantly affect Na^+ absorption when applied in the apical or basolateral compartment (−1.2 ± 0.44 mM, $n = 12$; −1.3 ± 0.69 mM, $n = 6$). At variance, clofilium (10^{-4} M), an inhibitor of the I_{sK}/KvLQT1 channel, reduced by 50% this K^+ gradient to 0.73 ± 0.033 mM ($n = 6$) after a 24-h application (ANOVA, $p < 0.001$).

To more precisely examine rapid modifications of ionic transports in these cells, similar experiments were performed by studying the short-circuit current Isc under basal conditions or after a 30-min period of drug application (Fig. 4*B*). Under basal conditions, the short-circuit

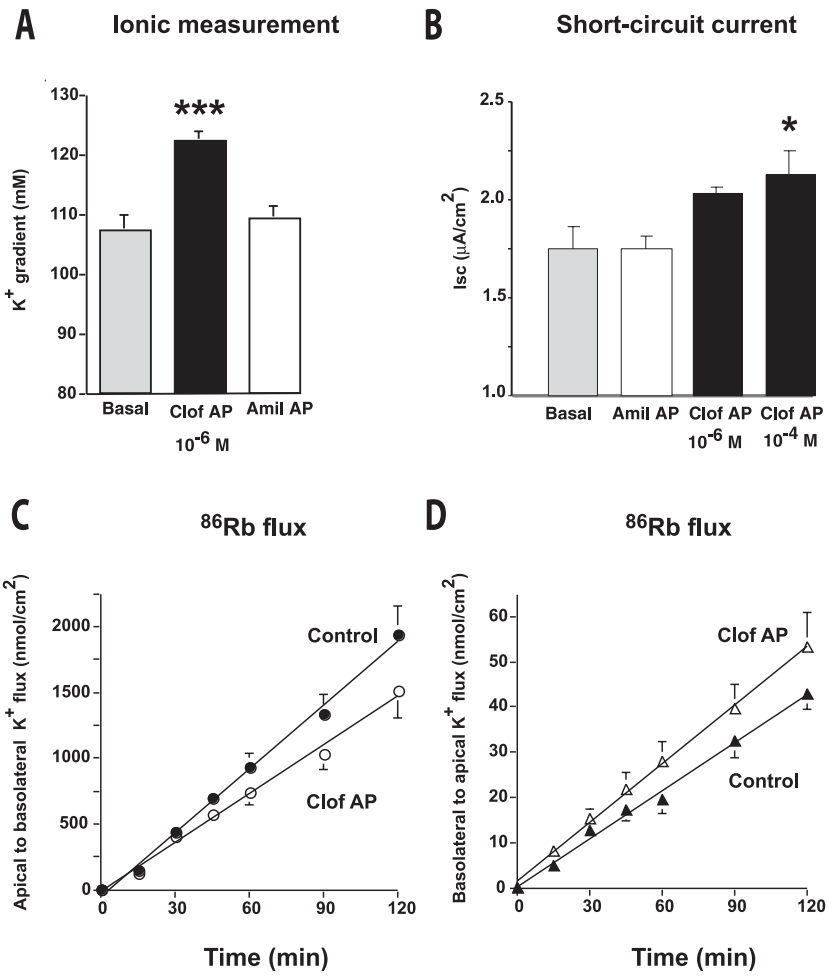

FIGURE 5. **Evidence for a K^+ transport in EC5v apically bathed with high K^+ solution.** In these series of experiments, cells were cultured on filters and placed with a low K^+ medium (4.2 mM) on the basolateral side and a high K^+ medium (160 mM) on the apical side for a 24-h period. Clofilium (*Clof*, inhibitor of I_{sK}/KvLQT1 channel, 10^{-4} and 10^{-6} M) and amiloride (*Amil*, 10^{-4} M) were added to the apical compartment. *A*, secretion of K^+. When the cells were cultured on filters for a 24-h period in such non-symmetrical K^+ conditions, they were able to maintain a high K^+ gradient (107 ± 3.0 mM, $n = 11$). This gradient was increased when clofilium (10^{-6} M, $p < 0.001$) was added in the apical medium, but was not altered by the presence of apical amiloride. *B*, short-circuit current. In basal conditions, the short-circuit current was 1.7 ± 0.11 $\mu A/cm^2$ ($n = 6$). This current was increased by a 30-min apical application of 10^{-4} M clofilium ($p < 0.001$, ANOVA). Apical amiloride did not alter Isc. *C*, calculated apical to basolateral transepithelial K^+ flux with ^{86}Rb determination in the presence of apical clofilium (10^{-4} M). When ^{86}Rb was added in the apical compartment and measured in the basolateral one (apical to basolateral flux), the radioactivity increased in the basolateral compartment as a function of time following the equation: $y = 16.2\,x - 47.0$ ($r^2 = 0.996$, means of 12 independent determinations), where y is in nanomole/cm^2 and x is in minutes. In the presence of apical clofilium, the equation was $y = 12.3\,x - 8.4$ ($r^2 = 0.996$, means of 6 independent determinations, difference between the slopes: $p < 0.001$). *D*, calculated basolateral to apical transepithelial K^+ flux with ^{86}Rb determination in the presence of apical clofilium (10^{-4} M). When ^{86}Rb was added in the basolateral compartment and measured in the apical one (basolateral to apical flux), the radioactivity increased in the apical compartment as a function of time following the equation: $y = 0.35\,x + 0.26$ ($r^2 = 0.993$, means of 6 independent determinations), where y is in nanomole/cm^2 and x is in minutes. In the presence of apical clofilium, the equation was $y = 0.43\,x + 1.39$ ($r^2 = 0.998$, means of 6 independent determinations, difference between the slopes: $p < 0.001$).

current Isc was 1.9 ± 0.13 $\mu A/cm^2$ ($n = 12$), and the transepithelial potential was +1.6 ± 0.19 mV ($n = 12$), basolateral side positive. These results suggest the presence of a net secretion of negative charges toward the apical side or a net absorption of positive charges toward the basolateral side, presumably Na^+, since a net K^+ secretion was observed in these conditions (see above). This possible Na^+ transport was not inhibited by apical amiloride (Isc: 2.0 ± 0.06 $\mu A/cm^2$, $n = 3$). In contrast, Isc decreased after a 30-min basolateral application of ouabain (0.88 ± 0.108 $\mu A/cm^2$, $n = 6$, ANOVA, $p < 0.001$) or, at variance to that observed above, after application of bumetanide (1.3 ± 0.22 $\mu A/cm^2$, $n = 6$, ANOVA, $p < 0.05$). Apical ouabain, or bumetanide had no effect (data not shown). Apical clofilium (10^{-4} M) decreased Isc (1.2 ± 0.03 $\mu A/cm^2$, $n = 6$, ANOVA, $p < 0.05$).

Another approach to investigate the K^+ transport was the measurement of unidirectional transepithelial K^+ flux with ^{86}Rb determination under basal conditions during a 120-min period (Fig. 4*C*). When ^{86}Rb was added in the basolateral compartment and measured in the apical side (basolateral to apical flux), the radioactivity increased in the apical compartment as a function of time following the equation: $y = 0.40\,x - 1.25$ ($r^2 = 0.998$, means of 39 independent determinations), where y is in nanomole/cm^2 and x is in minutes. On the opposite, when ^{86}Rb was added in the apical compartment and measured in the basolateral one (apical to basolateral flux), the radioactivity increased in the basolateral compartment as a function of time following the equation: $y = -0.14 \times +0.14$ ($r^2 = 0.992$, means of 18 independent determinations), where y is in nanomole/cm^2 and x is in minutes. The K^+ transport from the basolateral side to the apical one was clearly higher than the reversed one, from the apical to the basolateral sides (slope comparison, $p < 0.001$), confirming the existence of a net K^+ secretion flux. In the presence of ouabain (10^{-4} M), or bumetanide (10^{-4} M), applied in the basolateral compartment, a significant decrease of the basolateral to apical K^+ flux was observed (Fig. 4*D*). The calculated slopes for basolateral to apical K^+ flux were 0.42 ± 0.049 *versus* 0.23 ± 0.041 nmol/cm^2/min for control and ouabain-treated cells, respectively (means of 18 independent determinations, *t* test: $p < 0.001$), and 0.44 ± 0.047 *versus* 0.30 ± 0.038 nmol/cm^2 for control and bumetanide-treated cells, respectively (means of 15 independent determinations, *t* test: $p < 0.05$). In the presence of 10^{-4} M apical clofilium, no significant decrease of K^+ flux was observed (slopes: 0.49 ± 0.069 nmol/cm^2/min, and 0.43 ± 0.066 nmol/cm^2/min for control and clofilium-treated cells, respectively, means of 9 independent determinations).

In conclusion of this series of experiments, EC5v cells are able to secrete K^+ by a mechanism that is dependent of a basolateral Na^+, K^+-ATPase and Na-K-2Cl cotransport, and, at least, of KvLQT1, depending of the experimental procedure. This K^+ secretion was associated with a Na^+ absorption that was not mediated by an amiloride-sensitive ENaC channel.

EC5v Cells Absorb Potassium via I_{sK}/KvLQT1 Channel When Apically Bathed with High K^+ Solution—Because *in vivo*, in adult animals, semicircular canal cells are bathed at their apical side with endolymph, a high K^+, low Na^+ fluid, we examined whether EC5v cells are able to sustain a high K^+ gradient between the apical and basolateral compartments.

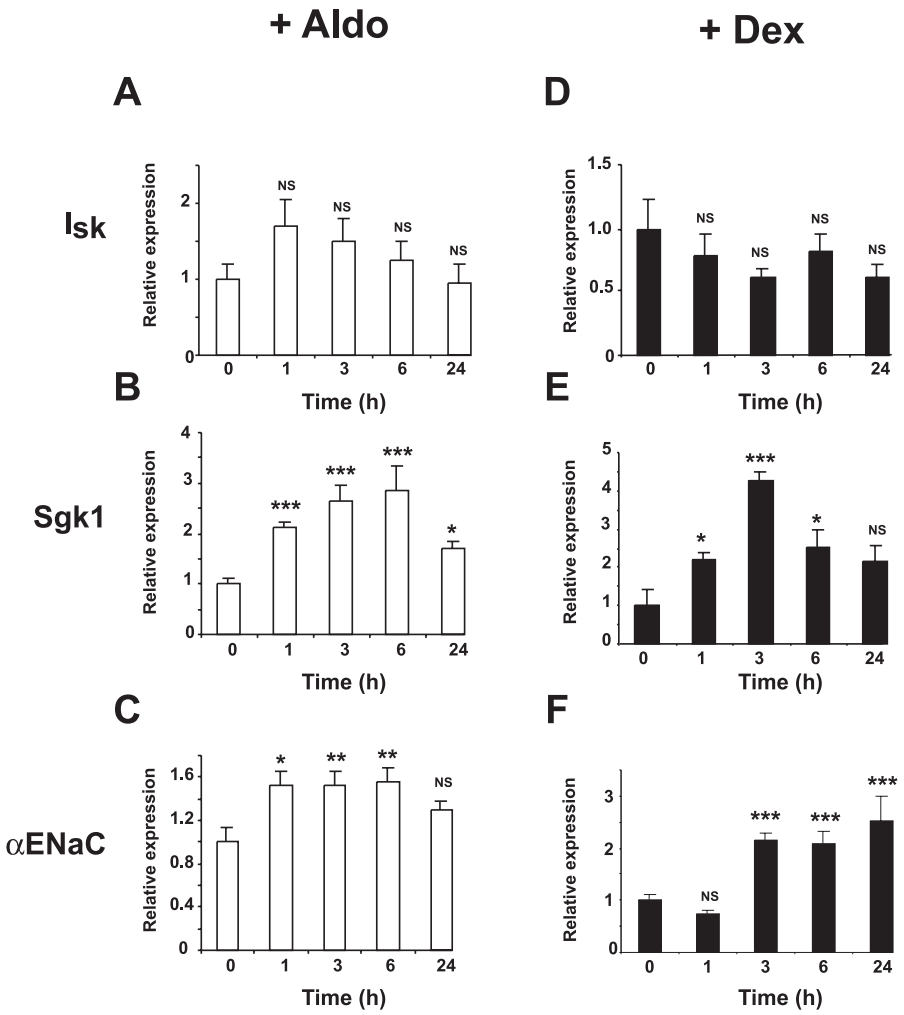

FIGURE 6. **Regulation of I_{sK}, sgk1, and αENaC expression by corticosteroid hormones.** Real time PCR analysis of I_{sK} (*A* and *D*), Sgk1 (*B* and *E*), and αENaC (*C* and *F*) mRNA expression was performed in EC5v cells after aldosterone (*A–C*) or dexamethasone (*D–F*) treatment. Highly differentiated vestibular EC5v cells were grown on filters for 24 h in minimum medium and subsequently treated for various periods of time (0, 1, 3, 6, or 24 h) with 10 nM aldosterone or 100 nM dexamethasone. Results were normalized by the amplification of the 18 S rRNA and were expressed as relative -fold induction compared with basal conditions set at 1. Each point represents the mean ± S.E. of at least three independent determinations performed in duplicate. Statistical significance: *, $p < 0.05$; **, $p < 0.01$; and ***, $p < 0.001$, compared with basal values (time 0), *NS*, not significant.

In this series of experiments, cells were cultured on filters and placed with a low K^+ medium (4.2 mM) on the basolateral side and a high K^+ medium (160 mM) on the apical side (Fig. 5). After a 24-h period, the cells were able to maintain a relatively high K^+ gradient (107 ± 3.0 mM, $n = 11$). This gradient was significantly increased to 122 ± 1.8 mM ($n = 12$) when clofilium (10^{-6} M) was added to the apical medium ($p < 0.001$) (Fig. 5*A*). This K^+ gradient (Fig. 5*A*) as well as its associated Na^+ gradient (84 ± 4.1 mM, $n = 12$) were not altered by the presence of apical amiloride (10^{-5} M) (88 ± 2.6 mM, $n = 12$).

The short-circuit current was 1.8 ± 0.11 μA/cm^2 ($n = 6$) under these basal conditions (Fig. 5*B*), and the transepithelial potential was +2.9 ± 0.22 mV ($n = 6$), basolateral side positive, a value that is significantly higher than in the presence of apical low K^+ medium ($p < 0.001$). Again, this result suggests the presence of a net secretion of negative charges toward the apical side or, more likely, a net absorption of positive charges (K^+) toward the basolateral side, considering the ionic gradients in this experimental condition. Isc was increased to 2.1 ± 0.12 ($n = 6$) after a 30-min apical application of 10^{-4} M clofilium ($p < 0.05$, ANOVA); the effect of 10^{-6} M clofilium (2.0 ± 0.033, $n = 3$) did not reach statistical significance. Apical amiloride (10^{-5} M) did not alter Isc.

In the presence of apical artificial high K^+ endolymph, the apical to basolateral ^{86}Rb fluxes were extremely high (Fig. 5*C*). The radioactivity increased in the basolateral compartment as a function of time with a slope of 16.2 ± 0.48 nmol/cm^2/min ($r^2 = 0.996$, means of 6 independent determinations). This K^+ flux decreased (slope 12.3 ± 0.48 nmol/cm^2/min; $r^2 = 0.993$; $p < 0.001$) with apical exposure to clofilium. Conversely, the basolateral to apical K^+ flux (slope 0.35 ± 0.013 nmol/cm^2/min; $r^2 = 0.993$, means of 6 independent determinations) was increased in the presence of apical clofilium (slope 0.43 ± 0.010 nmol/cm^2/min; $r^2 = 0.998$; $p < 0.001$) (Fig. 5*D*), consistent with the inhibition of the apical I_{sK}/KvLQT1 potassium channel function. These results indicate that, in the presence of high K^+ concentration at the apical side of the epithelium, the apical I_{sK}/KvLQT1 channel is involved in the absorption of K^+ from the apical to the basolateral side of the EC5v cell line.

Transcriptional Regulation of Na^+ and K^+ Transporters—Given the presence of MR and GR in EC5v cells, we next examined the effects of aldosterone and dexamethasone on the expression of I_{sK}, Sgk1 (serum and glucocorticoid-regulated kinase 1), and the α subunit of ENaC. Aldosterone (10^{-8} M) did not significantly modify I_{sK} mRNA levels (Fig. 6*A*), whereas it rapidly induced the expression of Sgk1 (Fig. 6*B*) and αENaC (Fig. 6*C*) as early as 1 h after hormonal treatment, the mRNA levels remained high for 6 h. A similar pattern was observed after dexamethasone exposure (Fig. 6, *D–F*). I_{sK} mRNA levels were not modified after glucocorticoid treatment (Fig. 6*D*) that, however, rapidly increased Sgk1 mRNA (Fig. 6*E*); the induction of the expression of αENaC was somehow delayed after 1–3 h of hormonal stimulation and remained significant after 6–24 h, suggesting a more sustained stimulation of ENaC (Fig. 6*F*). Altogether, these results clearly demonstrate that EC5v cells possess all the necessary molecular components for corticosteroid hormone actions. These vestibular cells respond to mineralocorticoids and glucocorticoids, which both stimulate the expression of important compo-

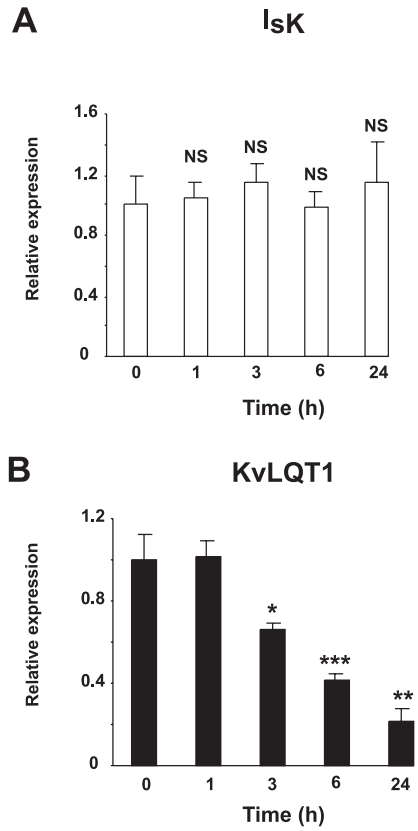

FIGURE 7. **Effect of high apical K^+ concentration on I_{sK} and KvLQT1 mRNA.** Real time PCR analysis of I_{sK} (*A*) or KvLQT1 (*B*) mRNA expression was performed in EC5v cells after 1–24 h exposure to apical high K^+ concentration and basolateral epithelial medium. Results were normalized by the amplification of the 18 S rRNA and expressed as relative -fold induction compared with basal conditions set at 1. Each point represents the mean ± S.E. of at least three independent determinations performed in duplicate. Statistical significance: *, $p < 0.05$; **, $p < 0.01$; and ***, $p < 0.001$, compared with basal values (time 0), *NS*, not significant.

nents of transepithelial sodium transport. In contrast, genes encoding for the I_{sK}/KvLQT1 channel do not seem to be directly regulated by aldosterone or glucocorticoids in this cellular model. However, in the presence of apical high K^+ concentration, whereas the levels of I_{sK} transcripts did not vary (Fig. 7*A*), expression of KvLQT1 mRNA was progressively and significantly reduced as early as 3 h after high K^+ exposure, and reached ~30% of its initial value after 24 h (Fig. 7*B*), suggesting that the composition of the apical fluid tightly controlled the K^+ transporter gene transcription.

DISCUSSION

The present study aimed at generating and characterizing an inner ear secretory cell line derived from transgenic mice expressing the immortalizing SV40 large T antigen under the control of the P1 promoter of the mineralocorticoid receptor. EC5v cells originating from the ampulla of a semicircular canal exhibited characteristic features of polarized epithelial cells. Importantly, these cells are able to generate a small K^+ gradient between their apical and basolateral sides, such a gradient being dependent on the apical I_{sK}/KvLQT1 channel, the basolateral Na^+, K^+-ATPase pump, and Na-K-2Cl cotransport. The three subunits of ENaC are also detected at both mRNA and protein levels, the expression of the α subunit being clearly stimulated by aldosterone and dexamethasone treatment. However, the implication of ENaC in vectorial sodium transport across the epithelium remains to be elucidated. Thus, this new cellular model appears to be a unique experimental system and a suitable tool to study the regulation of K^+ homeostasis in the inner ear, at the cellular and molecular level.

Generation of an Inner Ear Cell Line by Targeted Oncogenesis Strategy Using MR Promoter—Targeted oncogenesis is known to be an appropriate strategy to develop novel cell lines (22–24). In our hands, this experimental approach allowed us to establish several interesting cell lines originating from various aldosterone-sensitive tissues, among them the distal nephron (17), the brown adipocytes (18), and others. Because of the presence of MR in the inner ear secretory structures, and given the proposed regulatory effects of aldosterone on endolymph secretion (see below), we chose the same strategy in which the proximal promoter of the human MR gene drove the expression of the SV40 large T antigen, to generate a new immortalized cell line derived from the semicircular canal. Indeed, the expression of this immortalizing oncogene is restricted to MR-expressing cells that are able to activate this tissue-specific promoter thus maintaining both their proliferation and differentiation.

MR have been detected in different structures of the cochlea (organ of Corti, stria vascularis, spiral ligament, and spiral ganglion cells) (25, 26). *In vitro*, in the stria vascularis, aldosterone was shown to induce a rapid (within seconds) and transient decrease of the short-circuit current, suggesting a non-genomic effect; it should be noted that, under the same experimental conditions, corticosteroid hormones induced an increase in the short-circuit current (27). In the vestibule, only a few studies have been performed but specific aldosterone binding has been reported to be in the same order of magnitude as in the cochlea (16, 28). Moreover, 11β-hydroxysteroid dehydrogenase has been detected in the dark cells of the ampulla of semicircular canal by histochemical techniques (29). Finally, it has been proposed that the absence of circulating aldosterone led to an ultrastructural alteration of the dark cells membranes (30).

The implication of aldosterone in the pathogenesis of inner ear diseases has been postulated. Indeed, aldosterone administration is known to induce an endolymphatic hydrops (31), an increase in endolymph volume, which is the anatomical substratum for Menière disease. Nevertheless, no modification in plasma aldosterone concentration was observed in Menière patients during the attack-free period (32). At variance, in aged patients (above 58 years old), a recent study demonstrated that higher aldosterone levels correlated with better hearing. Thus, the cochlea might be the target for such a possible protective effect of aldosterone on hearing (33).

Cell Model of Endolymph Secretion—Because the inner ear is small, complex, and encased in bone, cell culture would provide an invaluable tool to study, at the cellular level the mechanisms and the regulation of ion transports in endolymph. Nevertheless, this technique remains difficult in terms of cell types and their differentiation stages. The majority of the cell lines are immortalized with a conditionally expressed, temperature-sensitive variant of the SV40 large T antigen (for review, see Ref. 34). If we consider cell lines derived from endolymph secretory epithelium (stria vascularis in the cochlea, and dark cells in the vestibule), only a few data are available, reporting dome formation, tight junctions, and, in some cases, the presence of "specific" proteins such as I_{sK} (35). Another cellular model is the primary culture of marginal cells from gerbils immortalized by E6/E7 genes of human papilloma virus (MCPV-8); electrophysiological studies provided evidence for apical barium-sensitive K^+ channel, and amiloride-sensitive Na^+ channel (14), these currents were dependent on cAMP (36).

Given the histology of the ampulla of the semicircular canal, four cell types could be obtained: sensory-ciliated cells, transitional cells, dark cells, and the so-called undifferentiated cells. It is known that sensory cells are unable to proliferate and the electron microscopy features of EC5v cells clearly evoked dark cells or transitional cells. Dark cells are

known to possess apical I_{sK}/KvLQT1 channel and basolateral Na^+, K^+-ATPase and Na-K-2Cl cotransporter, which have been clearly identified in EC5v cells. *Ex vivo*, preparation of dark cell sheets exhibited a 100 times lower transepithelial resistance than that observed for EC5v cells (37). Very little is known concerning the characterization of the transitional cells and their putative role (38). Nevertheless, it is unlikely that EC5v cells represent transitional cells given the lack of amiloride effect (38). Finally, undifferentiated cells that cover the upper part of the ampulla as well as the entire semicircular canal are flat cells, linked by tight junctions. These cells have been cultured from 4-day-old Wistar rats (39); they displayed electrophysiological properties (R_T = ~3300 $\Omega \times cm^2$; V_T = ~−4 mV; Isc = ~1.5 $\mu A/cm^2$) and a K^+ secretion (16–32 $nmol/cm^2/h$) of the same order of magnitude as those described for EC5v cells in the present study. Nevertheless, I_{sK}/KvLQT1 has not been identified in these undifferentiated cells (40). Altogether, we propose that EC5v cells could represent dark cells thus constituting an appropriate cellular model to further explore the regulatory mechanisms of endolymph secretion.

EC5v Cells Secrete Potassium and Absorb Sodium under Low Apical Potassium Conditions—The functional properties of EC5v cells have been examined in two experimental conditions. The symmetric condition in which both apical and basolateral sides were bathed with low K^+ and high Na^+ concentrations reminiscent of perilymphatic fluid, thus mimicking for instance, the maturation of endolymph during early developmental stages (41), or pathological situations such as a rupture of the Reissner membrane that could be observed in Menière disease (42). The second experimental condition that reproduces the physiological endolymphatic environment was achieved by exposing the apical side of the cells to a high K^+, low Na^+ medium. When EC5v cells were bathed with low K^+ concentration on both sides for 24 h, they were able to generate a K^+ gradient of 1.5 mM, a value in agreement with the calculated ^{86}Rb flux (approximately 30 $nmol/cm^2/h$), ^{86}Rb being assumed to mimic K^+ fluxes via the same transporters with very similar kinetic parameters. In an *ex vivo* preparation of freshly isolated semicircular canal, in similar symmetrical conditions, the K^+ flux was estimated to be 1 order of magnitude higher (43). Even though this K^+ gradient is lower than that observed *in vivo*, these cells are able to secrete K^+ and to maintain a transepithelial ionic gradient.

Considering the effects of various drugs tested, it is obvious that the Na^+, K^+-ATPase and Na-K-2Cl cotransporter are located at the basolateral side of these cells and thus facilitate K^+ entry into the cell. Indeed, their specific inhibitors, ouabain and bumetanide, inhibited ^{86}Rb flux and decreased the short-circuit current. The absence of bumetanide effect on the K^+ gradient after 24 h may be due to an escape of the drug effect or a compensatory action of the Na^+, K^+-ATPase. The presence of a functional I_{sK}/KvLQT1 channel was demonstrated at the apical side of the epithelium, presumably responsible of this K^+ secretion. Indeed, clofilium an inhibitor of this channel known to decrease the endocochlear potential (44), inhibited K^+ gradient and decreased Isc. This decrease in the short-circuit current that reflected the resultant vectorial ionic currents (both positive and negative ions, basolateral to apical and apical to basolateral) through the epithelium, could be related to the inhibition of the basolateral transporters (Na^+, K^+-ATPase and Na-K-2Cl cotransporter) because of an increase of the intracellular K^+ concentration. Surprisingly, clofilium failed to decrease ^{86}Rb flux, a finding that could be explained by the relatively low intensity of the flux measured under this experimental condition.

On the other hand, although EC5v cells expressed the amiloride-sensitive ENaC as demonstrated both by RT-PCR and Western blot, the α subunit of ENaC being regulated by aldosterone and dexamethasone, there is no experimental evidence for the involvement of this channel in Na^+ absorption. Indeed, amiloride failed to inhibit Na^+ gradient or short-circuit current whatever the composition of the apical fluid. The lack of effect of basolateral exposure of amiloride ruled out an inappropriate targeting of this channel to the basolateral membrane.

I_{sK}/KvLQT1 Channel Plays a Pivotal Role in Potassium Absorption under High Apical Potassium Conditions—We next examined the ionic transports under the "asymmetrical" conditions in which the apical pole of the cells was exposed during 24 h to an endolymph-like solution with high K^+ and low Na^+ concentrations, whereas a perilymph-like solution (low K^+ and high Na^+) was applied to the basolateral side, a situation that occurs in adult, normal inner ear. Importantly, EC5v cells were able to maintain a high K^+ gradient in this condition. Of interest, this K^+ gradient was higher when I_{sK}/KvLQT1 was inhibited by clofilium, strongly suggesting that this channel was clearly responsible for K^+ transport from the apical bath to the cellular compartment, following the transmembrane electrochemical gradient. The fact that I_{sK}/KvLQT1 is working inwardly in the presence of the high external K^+ concentration has been previously shown by patch clamp in dark cells (37). Furthermore, the effect of clofilium on the short-circuit current was the opposite of that observed in the symmetrical condition, as expected in the case of reversed flux through the I_{sK}/KvLQT1 channel. Finally, clofilium decreased the apical to basolateral ^{86}Rb flux that was ~30 times higher in the asymmetrical condition, and increased the basolateral to apical ^{86}Rb flux, a finding in accordance with this inward direction of the K^+ transport.

Regulation of I_{sK}/KvLQT1 is relatively well documented in cardiac cells. Indeed, elevated cAMP increased K^+ current (45), whereas the β-adrenergic system via the phosphorylation of protein kinase C, also regulated the amplitude of the I_{sK}/KvLQT1 current (46, 47). We provided evidence that both components of the I_{sK}/KvLQT1 channel are expressed in EC5v cells, but little information is known with respect to their functional coupling. The finding that KvLQT1 mRNA levels gradually decreased as a function of incubation time with the apical K^+-rich solution, whereas no modification in I_{sK} transcripts was observed, suggested independent regulatory pathways that remain to be further elucidated.

In summary, EC5v cells are a K^+-secreting, Na^+-absorbing cell line. They possess all the transporters known to be involved in endolymph secretion and thus represent an original experimental system to further investigate, at the cellular level, the regulation of these transport systems. In the future, EC5v cells should also constitute a suitable model to test drugs able to stimulate endolymph secretion to maintain normal hearing and balance.

Acknowledgments—We are indebted to Jacqueline Bauchet and the "Centre d'Exploration Fonctionnelle Intégrée" for ionic measurements, Nathalie Ialy-Radio for animal housing, and Cécile Pouzet who helped analyze confocal microscopy analyses. Finally, we thank Dr. Jacques Barhanin (CNRS UMR6097/UNSA, Valbonne, France) for helpful discussions and for providing the anti-I_{sK} and the KvLQT1 antibodies. We also thank Dr. Laurent Pascual-Le Tallec for critical reading of the manuscript.

REFERENCES

1. Ferrary, E., and Sterkers, O. (1998) *Kidney Int. Suppl.* **65,** S98–S103
2. Wangemann, P., Liu, J., and Marcus, D. C. (1995) *Hear. Res.* **84,** 19–29
3. Neyroud, N., Tesson, F., Denjoy, I., Leibovici, M., Donger, C., Barhanin, J., Faure, S., Gary, F., Coumel, P., Petit, C., Schwartz, K., and Guicheney, P. (1997) *Nat. Genet.* **15,** 186–189
4. Splawski, I., Tristani-Firouzi, M., Lehmann, M. H., Sanguinetti, M. C., and Keating, M. T. (1997) *Nat. Genet.* **17,** 338–340
5. Schulze-Bahr, E., Wang, Q., Wedekind, H., Haverkamp, W., Chen, Q., Sun, Y., Rubie,

C., Hordt, M., Towbin, J. A., Borggrefe, M., Assmann, G., Qu, X., Somberg, J. C., Breithardt, G., Oberti, C., and Funke, H. (1997) *Nat. Genet.* **17,** 267–268
6. Tyson, J., Tranebjaerg, L., Bellman, S., Wren, C., Taylor, J. F., Bathen, J., Aslaksen, B., Sorland, S. J., Lund, O., Malcolm, S., Pembrey, M., Bhattacharya, S., and Bitner-Glindzicz, M. (1997) *Hum. Mol. Genet.* **6,** 2179–2185
7. Vetter, D. E., Mann, J. R., Wangemann, P., Liu, J., McLaughlin, K. J., Lesage, F., Marcus, D. C., Lazdunski, M., Heinemann, S. F., and Barhanin, J. (1996) *Neuron* **17,** 1251–1264
8. Rivas, A., and Francis, H. W. (2005) *Otol. Neurotol.* **26,** 415–424
9. Mizuta, K., Iwasa, K. H., Tachibana, M., Benos, D. J., and Lim, D. J. (1995) *Hear. Res.* **88,** 199–205
10. Couloigner, V., Fay, M., Djelidi, S., Farman, N., Escoubet, B., Runembert, I., Sterkers, O., Friedlander, G., and Ferrary, E. (2001) *Am. J. Physiol.* **280,** F214–F222
11. Pondugula, S. R., Sanneman, J. D., Wangemann, P., Milhaud, P. G., and Marcus, D. C. (2004) *Am. J. Physiol.* **286,** F1127–F1135
12. Achouche, J., Liu, D. S., Tran Ba Huy, P., and Huy, P. T. (1991) *Ann. Otol. Rhinol. Laryngol.* **100,** 999–1006
13. Agrup, C., Berggren, P. O., Kohler, M., Spangberg, M. L., and Bagger-Sjoback, D. (1996) *Hear. Res.* **102,** 155–166
14. Tu, T. Y., Chiu, J. H., Yang, W. K., Chang, T. J., Yang, A. H., Shu, C. H., and Lien, C. F. (1998) *Hear. Res.* **123,** 97–110
15. Wangemann, P. (2002) *Audiol. Neurootol.* **7,** 199–205
16. Rarey, K. E., and Luttge, W. G. (1989) *Hear. Res.* **41,** 217–221
17. Le Menuet, D., Viengchareun, S., Muffat-Joly, M., Zennaro, M. C., and Lombes, M. (2004) *Mol. Cell. Endocrinol.* **217,** 127–136
18. Zennaro, M. C., Le Menuet, D., Viengchareun, S., Walker, F., Ricquier, D., and Lombes, M. (1998) *J. Clin. Investig.* **101,** 1254–1260
19. Le Menuet, D., Zennaro, M. C., Viengchareun, S., and Lombes, M. (2000) *Kidney Int.* **57,** 1299–1306
20. Blot-Chabaud, M., Laplace, M., Cluzeaud, F., Capurro, C., Cassingena, R., Vandewalle, A., Farman, N., and Bonvalet, J. P. (1996) *Kidney Int.* **50,** 367–376
21. Lesage, F., Attali, B., Lakey, J., Honore, E., Romey, G., Faurobert, E., Lazdunski, M., and Barhanin, J. (1993) *Receptors Channels* **1,** 143–152
22. Mellon, P. L., Windle, J. J., and Weiner, R. I. (1991) *Recent Prog. Horm. Res.* **47,** 69–93; 93–96
23. Briand, P., Kahn, A., and Vandewalle, A. (1995) *Kidney Int.* **47,** 388–394
24. Feunteun, J., Michiels, F., Rochefort, P., Caillou, B., Talbot, M., Fournes, B., Mercken, L., Schlumberger, M., and Monier, R. (1997) *Horm. Res.* **47,** 137–139
25. Yao, X., and Rarey, K. E. (1996) *Acta Otolaryngol.* **116,** 493–496
26. Furuta, H., Mori, N., Sato, C., Hoshikawa, H., Sakai, S., Iwakura, S., and Doi, K. (1994) *Hear. Res.* **78,** 175–180
27. Lee, J. H., and Marcus, D. C. (2002) *Audiol. Neurootol.* **7,** 100–106
28. Pitovski, D. Z., Drescher, M. J., and Drescher, D. G. (1993) *Hear. Res.* **69,** 10–14
29. Pitovski, D. Z. (1996) *Acta Otolaryngol.* **116,** 737–740
30. Ten Cate, W. J., and Rarey, K. E. (1991) *Arch. Otolaryngol. Head Neck Surg.* **117,** 96–99
31. Dunnebier, E. A., Segenhout, J. M., Wit, H. P., and Albers, F. W. (1997) *Acta Otolaryngol.* **117,** 13–19
32. Mateijsen, D. J., Kingma, C. M., De Jong, P. E., Wit, H. P., and Albers, F. W. (2001) *ORL J. Otorhinolaryngol. Relat. Spec.* **63,** 280–286
33. Tadros, S. F., Frisina, S. T., Mapes, F., Kim, S., Frisina, D. R., and Frisina, R. D. (2005) *Audiol. Neurootol.* **10,** 44–52
34. Rivolta, M. N., and Holley, M. C. (2002) *J. Neurobiol.* **53,** 306–318
35. Tu, T. Y., Chiu, J. H., Chang, T. J., Yang, A. H., and Lien, C. F. (1999) *Acta Otolaryngol.* **119,** 544–549
36. Tu, T. Y., Chiu, J. H., Shu, C. H., and Lien, C. F. (1999) *Hear. Res.* **127,** 149–157
37. Wangemann, P., Shen, Z., and Liu, J. (1996) *Hear. Res.* **100,** 201–210
38. Wangemann, P., and Shiga, N. (1994) *Am. J. Physiol.* **266,** C1046–C1060
39. Milhaud, P. G., Nicolas, M. T., Bartolami, S., Cabanis, M. T., and Sans, A. (1999) *Pflugers Arch.* **437,** 823–830
40. Nicolas, M., Dememes, D., Martin, A., Kupershmidt, S., and Barhanin, J. (2001) *Hear. Res.* **153,** 132–145
41. Anniko, M., Wroblewski, R., and Wersall, J. (1979) *Arch. Otorhinolaryngol.* **225,** 161–163
42. Paparella, M. M. (1985) *Acta Otolaryngol.* **99,** 445–451
43. Ferrary, E., Bernard, C., Oudar, O., Sterkers, O., and Amiel, C. (1989) *Am. J. Physiol.* **257,** F182–F189
44. Mori, N., Sakagami, M., Fukazawa, K., and Matsunaga, T. (1993) *Eur. Arch. Otorhinolaryngol.* **250,** 186–189
45. Potet, F., Scott, J. D., Mohammad-Panah, R., Escande, D., and Baro, I. (2001) *Am. J. Physiol.* **280,** H2038–H2045
46. Kathofer, S., Rockl, K., Zhang, W., Thomas, D., Katus, H., Kiehn, J., Kreye, V., Schoels, W., and Karle, C. (2003) *Naunyn-Schmiedeberg's Arch. Pharmacol.* **368,** 119–126
47. Bosch, R. F., Schneck, A. C., Kiehn, J., Zhang, W., Hambrock, A., Eigenberger, B. W., Rub, N., Gogel, J., Mewis, C., Seipel, L., and Kuhlkamp, V. (2002) *Cardiovasc. Res.* **56,** 393–403

Functional I_{sK}/KvLQT1 Potassium Channel in a New Corticosteroid-sensitive Cell Line Derived from the Inner Ear

Marie Teixeira, Say Viengchareun, Daniel Butlen, Chrystophe Ferreira, Françoise Cluzeaud, Marcel Blot-Chabaud, Marc Lombès and Evelyne Ferrary

J. Biol. Chem. 2006, 281:10496-10507.
doi: 10.1074/jbc.M512254200 originally published online February 13, 2006
